RSC Advances

PAPER

View Article Online
View Journal | View Issue

Cite this: *RSC Adv.*, 2019, **9**, 22348

A real-time ratiometric fluorescent probe for imaging of SO_2 derivatives in mitochondria of living cells†

Junwei Shi, Wei Shu, Yong Tian, Yulong Wu, Jing Jing,* Rubo Zhang* and Xiaoling Zhang*

Received 29th April 2019
Accepted 20th June 2019

DOI: 10.1039/c9ra03207j

rsc.li/rsc-advances

A real-time ratiometric fluorescent probe (**IN-CZ**) for highly selective detection of sulfite was designed and synthesized, which is based on modulating the intramolecular charge transfer (ICT) of the hemicyanine dye platform. The mechanism of using the probe is mainly through the Michael addition that occurs between **IN-CZ** and sulfite with a detection limit of 2.99×10^{-5} M. **IN-CZ** displays a fast response (within 1 minute) and is highly selective for SO_3^{2-}/HSO_3^- over ROS, biologically relevant ions, biological mercaptans and other reactive species. More importantly, **IN-CZ** was suitable for ratiometric fluorescence imaging in living cells, by real-time monitoring of SO_3^{2-}/HSO_3^- changes in mitochondria targeted in living cells.

1. Introduction

Sulfur dioxide (SO_2) is an inevitable product from the combustion of coal and fossil fuels as well automobile exhausts, causing a serious threat to the ecological environment and human health.[1] In general, SO_2 is inhaled into the human body through the respiratory tract, and then it mainly exists in a two anions equilibrium state, sulfite and bisulfite (SO_3^{2-}/HSO_3^-) in physiological systems.[2] Of which, sulfite has been widely used as an antioxidant in food, beverages, pharmaceuticals and preservatives.[3] However, prolonged exposure to excessive SO_2 may cause respiratory tract infection, even leading to lung cancer, cardiovascular disease and neurological disorders.[4] SO_2 and its derivatives (SO_3^{2-}/HSO_3^-) can alter the intracellular thiol levels, and then destroy the redox balance in the cells leading to neuron disorders.[5] Mitochondria as the main place for energy supply and transformation, provide a large number of reactive oxygen species (ROS) and reactive sulfur species (RSS).[6] Moreover, in the process of energy supply and transformation in mitochondria of cells, SO_2 and its derivatives (SO_3^{2-}/HSO_3^-) can also be produced from L-cysteine in reactions catalyzed by aspartate aminotransferase-2. The abnormal endogenous levels of SO_2 and its derivatives (SO_3^{2-}/HSO_3^-) can also cause a series of pathological changes.[7] The United Nations Food and Agriculture Organization (FAO) and The World Health Organization (WHO) have regulated an acceptable daily intake of sulfite to be lower than 0.7 mg kg^{-1} of body weight.[8] Thus, developing methods to detect exogenous and endogenous SO_2 and its derivatives (SO_3^{2-}/HSO_3^-) is of great significance.

At present, there are many detection strategies for SO_3^{2-}/HSO_3^-, including Monier-Williams,[9] electrochemical,[10] fluorescence spectrophotometry,[11] chromatography,[12] capillary electrophoresis,[13] titration[14] and fluorescent probe.[15] Among which, fluorescent indicators for SO_3^{2-}/HSO_3^- have attracted much attention due to their apparent advantages over other methods, such as high selectivity and specificity, operational simplicity, as well as high space–time resolution real-time detection and imaging *in vivo*.[16] As SO_3^{2-}/HSO_3^- is mainly expressed in mitochondria of cells, the quantitative detection of SO_3^{2-}/HSO_3^- is of great importance in both chemical and mitochondria targeted in living cells.[17]

In this work, we designed and synthesized a new ratiometric fluorescent probe **IN-CZ** for real-time monitoring of SO_3^{2-}/HSO_3^- changes in mitochondria targeted in living cells. The synthesis route for **IN-CZ** is shown in Scheme 1. The Michael addition that occurs between **IN-CZ** and sulfite makes the conjugate structure change (as shown in Scheme 2). The probe can not only realize ratiometric detection of SO_3^{2-}/HSO_3^-, but also shows high selectivity and sensitivity for SO_3^{2-}/HSO_3^- against various interferences with a detection limit of 2.99×10^{-5} M. **IN-CZ** exhibits excellent stability and localizes well in the mitochondria. Moreover, **IN-CZ** displayed a fast response (within 1 minute) and lower cell toxicity, which endows **IN-CZ** with good permeability and application to imaging SO_3^{2-}/HSO_3^- in living cells.

Key Laboratory of Cluster Science of Ministry of Education, Beijing Key Laboratory of Photoelectronic/Electrophotonic Conversion Materials, School of Chemistry and Chemical Engineering, Beijing Institute of Technology, Beijing 100081, P. R. China. E-mail: zhangxl@bit.edu.cn; zhangrubo@bit.edu.cn; hellojane@bit.edu.cn; Fax: +86-10-88875298; Tel: +86-10-88875298

† Electronic supplementary information (ESI) available. See DOI: 10.1039/c9ra03207j

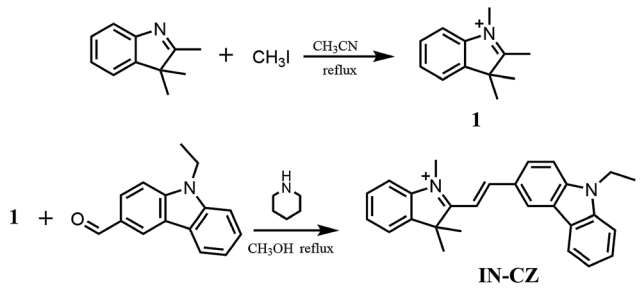

Scheme 1 Synthesis route for **IN-CZ**.

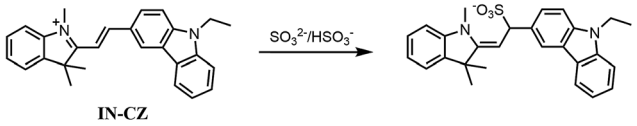

Scheme 2 Proposed sensing mechanism of **IN-CZ** towards SO_3^{2-}/HSO_3^-.

2. Experimental

2.1 Materials and instruments

All the chemicals and reagents were obtained from commercial suppliers and prepared in stock with standard methods before use. Silica gel (200–300 mesh, Qingdao Haiyang Chemical Co.) was used for column chromatography. NMR spectra were recorded on a Bruker Advance III at 400 MHz for ^{1}H NMR and at 100 MHz for ^{13}C NMR with chemical shifts reported as ppm (in $CDCl_3$, TMS as internal standard). Mass spectra (MS) were measured with a Bruker Apex IV FTMS using electrospray ionization (ESI†). Absorption spectra were recorded on a Purkinje TU-1901 spectrophotometer. Fluorescence measurements were taken on a Hitachi F-7000 fluorescence spectrometer with a 10 mm quartz cuvette. Excitation wavelength was 420 nm.

2.2. Synthesis of fluorescent probe IN-CZ

2.2.1 Synthesis of compound 1. In 10 mL of acetonitrile, 2,3,3-trimethylindolenine (1.0 g, 6.3 mmol) and iodomethane (4.43 g, 31.4 mmol) were added, the mixture was stirred and refluxed overnight. Afterwards, cooling to room temperature (RT), the mixture was filtered and pink solid **1** was obtained.

2.2.2 Synthesis of compound IN-CZ. In 1 mL of piperidine and 25 mL of ethanol, a mixture of compound **1** (215 mg, 0.75 mmol) and *N*-ethyl-3-carbazolecarboxaldehyde (167 mg, 0.75 mmol) was stirred at 80 °C for 24 h. Afterwards, the mixture was extracted with DCM (30 × 3 mL) and washed with water (50 × 3 mL). The residue was purified by silica gel column chromatography using DCM/methanol (v/v, 30/1) as eluent to give white solid **IN-CZ**. ^{1}H NMR (DMSO-d_6, 400 MHz, TMS), δ (ppm): 9.10 (s, 1H), 8.64 (d, J = 7.82 Hz, 1H), 8.38 (d, J = 7.78 Hz, 1H), 8.24 (d, J = 6.5 Hz, 1H), 7.86 (t, J = 7.93 Hz, 3H), 7.72–7.68 (m, 2H), 7.63–7.58 (m, 3H), 7.38 (t, J = 6.23 Hz, 1H), 4.58–4.53 (m, 2H), 4.15 (t, J = 6 Hz, 3H), 1.85 (s, 6H), 1.38 (t, J = 8.1 Hz, 3H). ^{13}C NMR (100 MHz, $CDCl_3$), δ (ppm): 181.12, 156.94, 144.09, 142.52, 141.51, 140.64, 130.47, 129.38, 128.83, 127.17, 126.57, 125.42, 124.38, 123.45, 122.44, 122.36, 121.12, 110.76, 109.85, 108.94, 51.76, 38.15, 36.72, 27.43, 13.91. MALDI-MS (m/z): 379.216 for [M^+].

2.3 General procedure for analysis

Parent stock solution of fluorescent probe **IN-CZ** (10 mM) was prepared in absolute DMSO, and stored at 5 °C in a refrigerator as standby application. The various testing species were prepared from NaBr, NaCl, NaClO, Cys, Hcy, GSH, $FeCl_3$, $FeCl_2$, $NaNO_2$, $NaNO_3$, $NaHSO_4$, $NaHCO_3$ and $NaHSO_3$, and the stock solution concentrations of various species (10 mM) were prepared in twice-distilled water. The test solutions of **IN-CZ** (10 μM) were prepared by placing 100 μL of the corresponding stock solution into 100 mL PBS (10 mM, pH = 7.4). PBS solution was prepared with Na_2HPO_4 and KH_2PO_4, and adjusted to pH 7.4.

2.4 Determination of detection limit

According to the relevant literature published,[18] the detection limit was calculated based on the fluorescence titration. Fluorescence titration was carried out in the aqueous buffer (10 mM PBS, pH = 7.4) to determine the detection limit, which was calculated with the following equation:

$$\text{Detection limit} = 3\sigma/k$$

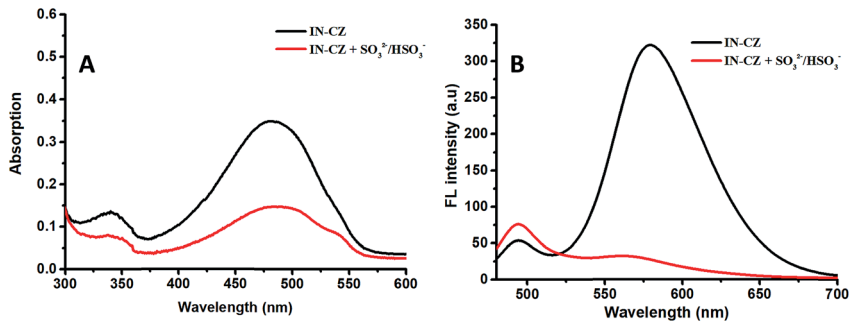

Fig. 1 Spectroscopic properties of **IN-CZ** (10 μM) in PBS buffer (pH = 7.4, PBS = 10 mM). (A) UV-vis absorption response of **IN-CZ** (10 μM) in the presence of SO_3^{2-}/HSO_3^- (10 μM). (B) Fluorescence emission intensity change of **IN-CZ** (10 μM) in the presence of SO_3^{2-}/HSO_3^- (100 μM). Excitation at 420 nm.

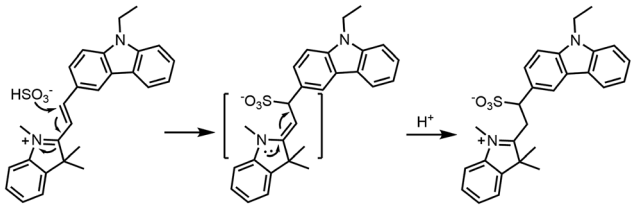

Scheme 3 Proposed reaction mechanism of **IN-CZ** with SO_3^{2-}/HSO_3^-.

Where σ is the standard deviation of blank measurements, k is the slope between the fluorescence intensity *vs.* SO_3^{2-}/HSO_3^- concentration.

2.5 Cytotoxicity

HeLa cells were cultured in the DMEM in a 5% CO_2 humidity incubator at 37 °C. Cells were inoculated in 96-well plates at 5000 cells per plate. After overnight culture, the medium in each well was replaced by fresh medium containing different concentrations of **IN-CZ** (0, 5, 10, 15, 20, 25 μM). After 24 h, 3-(4,5-dimethylthiazol-2-yl)-2,5-diphenyltetrazolium bromide (MTT, 5 mg mL^{-1}, 20 μL) was added to each plate for 3 h. Then medium was discarded, DMSO (100 μL) was added to dissolve the MTT formazan crystals and cultured for another 4 h. The absorbance in proportion to viable cell count was directly measured using a Bio-Rad 680 ELISA reader at 570 nm and all the measurements were completed three times under the condition of blank control.

2.6 Fluorescence imaging of SO_3^{2-}/HSO_3^- in living cells

HeLa cells were grown on glass-bottom culture dishes in DMEM supplemented with 10% fetal bovine serum and 1% penicillin. The cells were incubated under an atmosphere of 5% CO_2 and 95% air at 37 °C for 24 h. Before use, the cells were washed with PBS buffer solution three times. For the experiment of imaging of $NaHSO_3$, cells were incubated with 100 μM of $NaHSO_3$ for 30 min at 37 °C. Afterwards, cells were washed three times with PBS-free DMEM, the pretreated cells were incubated in culture media with **IN-CZ** (5 μM) for an additional 10 min at 37 °C, and then washed with PBS (pH = 7.4) three times. Fluorescence imaging of HeLa cells was conducted with an Olympus IX81 confocal fluorescence microscope with excitation wavelength of 405 nm.

3. Results and discussion

3.1 Spectral response of IN-CZ to SO_3^{2-}/HSO_3^-

The absorption and fluorescence spectra of **IN-CZ** in the PBS buffer (pH = 7.4, PBS = 10 mM) were studied. We first explored the spectra changes in the absence and presence of SO_3^{2-}/HSO_3^-. As shown in Fig. 1, the probe displayed a major absorption band centered at 480 nm with a corresponding fluorescence emission peak at 579 nm. With the addition of $NaHSO_3$, the absorption intensity of the peak at 480 nm significantly receded, revealing that the structure of **IN-CZ** has changed. Meanwhile the emission peak at 579 nm significantly reduced, and the corresponding fluorescence emission peak at 494 nm enhanced. The main reason for the spectra change is attributed to a 1,4-addition reaction that occurs between **IN-CZ** and $NaHSO_3$, the C=C conjugation between hemicyanine and carbazole is broken by the attack of SO_3^{2-}/HSO_3^- to obtain a blue-emission which is attributed to carbazole. These results indicate that **IN-CZ** has potential as a ratiometric fluorescent indicator for detection of SO_3^{2-}/HSO_3^-.

3.2 Recognition mechanism of IN-CZ for SO_3^{2-}/HSO_3^-

The recognition mechanism of **IN-CZ** for SO_3^{2-}/HSO_3^- is presumably due to the 1,4-addition reaction that occurs between **IN-CZ** and $NaHSO_3$ (Scheme 3). In order to verify the sensing mechanism, high resolution mass spectrometry (HRMS) was utilized to provide evidence in the absence and

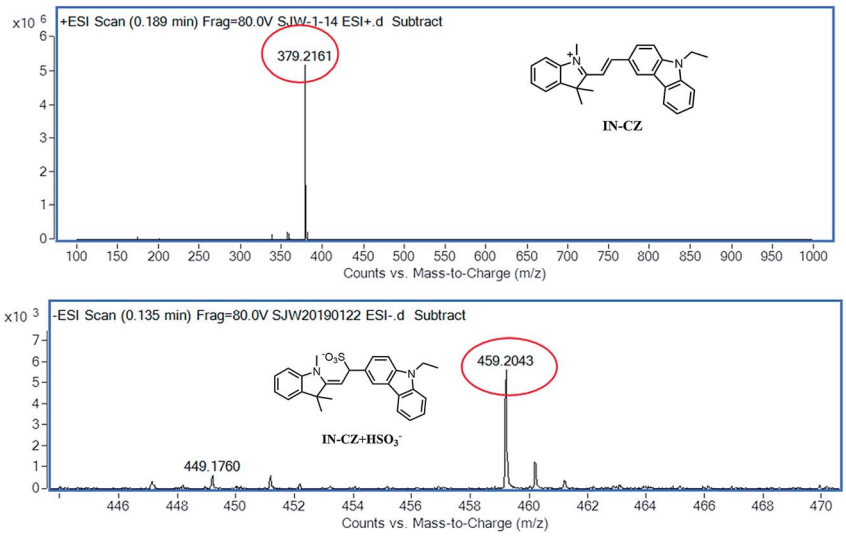

Fig. 2 HRMS spectra of probe **IN-CZ** treated without and with HSO_3^-.

presence of $NaHSO_3$ (as shown in Fig. 2). In the absence of $NaHSO_3$, HRMS of the probe in PBS buffer (pH = 7.4, PBS = 10 mM) was conducted and the peak exhibited at m/z = 379.2161. In the presence of $NaHSO_3$, the HRMS of the compound in PBS buffer (pH = 7.4, PBS = 10 mM) was conducted and the peak displayed at m/z = 459.2043, which is almost identical to the molecular weight of the adduct (calcd for $C_{27}H_{27}N_2O_3S$, m/z = 459.18). Both the literature and experimental results provide strong support for the proposed mechanism.[17e,f] The reaction changes the intramolecular charge transfer (ICT) of **IN-CZ**, and then a ratiometric fluorescent probe for detection of SO_3^{2-}/HSO_3^- was obtained.

3.3 The selectivity of IN-CZ for various analytes

To confirm the selectivity of **IN-CZ** towards HSO_3^-, the probe was incubated with various analytes. As shown in Fig. 3A, with the addition of Br^-, Cl^-, ClO^-, Hcy, Cys, GSH, HSO_4^{2-}, HCO_3^-, Fe^{2+}, Fe^{3+}, NO_2^-, NO_3^-, S^{2-}, CN^-, HS^- and $S_2O_3^{2-}$, there were nearly no fluorescence changes or weak fluorescence changes, with only SO_3^{2-}/HSO_3^- causing an obvious fluorescence change. Moreover, the probe was incubated with various analytes and HSO_3^- together. As shown in Fig. 3B, when other analytes coexist with HSO_3^-, the response of the probe to HSO_3^- was not affected. These results demonstrated that **IN-CZ** is not affected by these species and the emission of **IN-CZ** is stable in the presence of interference species; **IN-CZ** can detect SO_3^{2-}/HSO_3^- specifically.

Through selectivity and interference experiments, the photostability of **IN-CZ** was studied by continuous laser scanning at 420 nm. The fluorescence signal loss was calculated to be less than 3% over 30 min (Fig. S1†), indicating the excellent photostability of **IN-CZ**. Then, the kinetic profile of the recognition of **IN-CZ** for SO_3^{2-}/HSO_3^- was carried out, the response time of **IN-CZ** in the presence of $NaHSO_3$ was evaluated (Fig. S2†). When $NaHSO_3$ (50 μM) was added to the solution of **IN-CZ** (10 μM), the relative fluorescence of I_{494}/I_{579} increased immediately. This is consistent with the fact that the 1,4-addition reaction occurred between **IN-CZ** and $NaHSO_3$, making the probe conjugate structure change rapidly. The results above demonstrate the excellent photostability and sensitivity of **IN-CZ**.

3.4 Quantification of SO_3^{2-}/HSO_3^- and detection limit

The optical response validity of **IN-CZ** toward SO_3^{2-}/HSO_3^- was investigated. The fluorescence spectra of **IN-CZ** with various concentrations of $NaHSO_3$ (1, 2, 3, 4, 5, 6, 7, 8, 9, 10, 11, 12, 13, 14, 15, 16, 17, 18, 19, 20, 25, 30, 40, 50 μM) are shown in Fig. 4A.

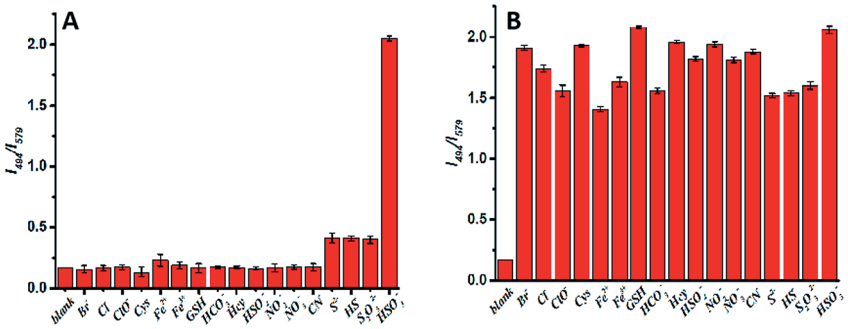

Fig. 3 (A) Relative fluorescence of **IN-CZ** (I_{494}/I_{579}) in the presence of various analytes. (B) Relative fluorescence of **IN-CZ** (I_{494}/I_{579}) towards $NaHSO_3$ (50 μM) when coexisting with various other analytes. (100 μM): Br^-; Cl^-; ClO^-; Hcy; Cys; GSH; HSO_4^{2-}; HCO_3^-; Fe^{2+}; Fe^{3+}; NO_2^-; NO_3^-; CN^-; S^{2-}; HS^-; $S_2O_3^{2-}$; SO_3^{2-}/HSO_3^- (50 μM) (except: GSH 1 mM, Hcy 1 mM, Cys 1 mM) in PBS buffer solution (pH = 7.4, PBS = 10 mM, **IN-CZ** = 10 μM). Excitation at 420 nm.

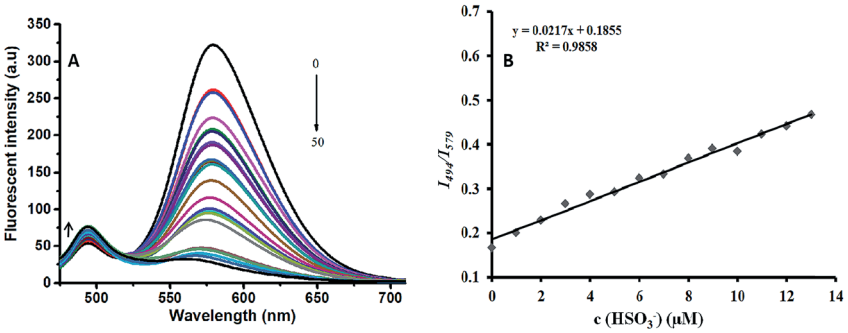

Fig. 4 (A) Fluorescence spectra of **IN-CZ** (10 μM) upon addition of $NaHSO_3$ (1, 2, 3, 4, 5, 6, 7, 8, 9, 10, 11, 12, 13, 14, 15, 16, 17, 18, 19, 20, 25, 30, 40, 50 μM). The reaction was performed in PBS buffer (pH = 7.4, 10 mM). (B) The linear relationship between the fluorescence intensity ratio of I_{494}/I_{579} and the SO_3^{2-}/HSO_3^- concentration (1, 2, 3, 4, 5, 6, 7, 8, 9, 10, 11, 12, 13 μM). The reaction was performed in PBS buffer (pH = 7.4, 10 mM). Excitation at 420 nm.

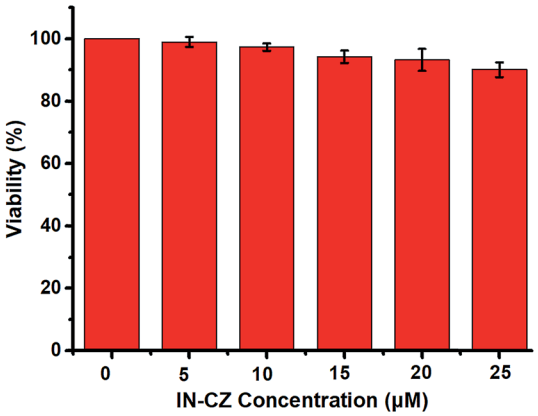

Fig. 5 Cytotoxicity assays for IN-CZ in HeLa cells. Cells were treated with different concentrations of probe IN-CZ for 24 h. Concentrations of IN-CZ (0 μM, 5 μM, 10 μM, 15 μM, 20 μM, 25 μM).

Upon gradually increasing the concentration of $NaHSO_3$, the fluorescence band centered at around 579 nm decreased immediately, and the fluorescence band centered at around 494 nm increased. The relative fluorescence intensity of I_{494}/I_{579} *vs.* the concentration of $NaHSO_3$ in the range of 1–13 μM was linear with a detection limit of 299 nM, as shown in Fig. 4B. Therefore, the probe **IN-CZ** is capable of the identification and quantification of SO_3^{2-}/HSO_3^-.

We also investigated the pH effect on the fluorescence spectrum of **IN-CZ** in the absence and presence of $NaHSO_3$ under a wider pH range (1–12). As shown in Fig. S3,† the spectral response of **IN-CZ** was evaluated in PBS buffer (pH = 7.4, 10 mM). The fluorescence intensity ratio (I_{494}/I_{579}) of the probe was barely affected in the pH range 5.0–10.0, which suggested that the probe was stable within this pH range. Afterwards, in the presence of $NaHSO_3$, the probe could respond to $NaHSO_3$ in the pH range 5.0–10.0, indicating that **IN-CZ** could be used for the detection of SO_3^{2-}/HSO_3^- under physiological conditions.

3.5 Cellular fluorescence imaging and cytotoxicity

To explore the application of **IN-CZ** in living cells, its cytotoxicity was evaluated in HeLa cells, using the 3-(4,5-dimethyl-2-thiazolyl)-2,5-diphenyltetrazolium bromide (MTT) assay under different probe concentrations. As displayed in Fig. 5, no significant change in the cell viability was observed when the cells were cultured in the presence of a high concentration of **IN-CZ** of 25 μM for 24 h. This indicates that **IN-CZ** shows no cytotoxicity and good biocompatibility in live cells.

To confirm the specific stain of mitochondria in living cells, we carried out a colocalization experiment (Fig. 6). HeLa cells were incubated with **IN-CZ** (5 μM) and Mito-tracker Red (100 nM, a commercial red-fluorescent mitochondrial dye) for 15 min at 37 °C, and the excess dye was washed away with

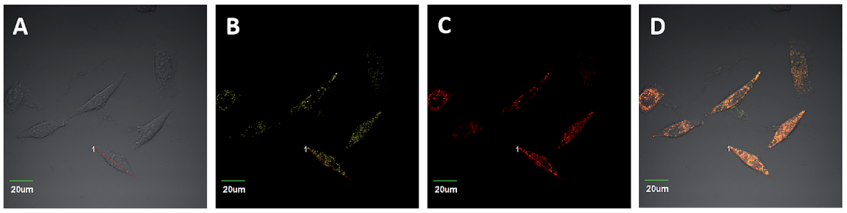

Fig. 6 HeLa cells were incubated with IN-CZ (5 μM) and Mito-Tracker Red (100 nM): (A) bright-field; (B) yellow channel of IN-CZ; (C) red-channel of Mito-Tracker Red; (D) merged images (B) and (C) in bright-field. Excitation at 405 nm. Scale bar: 20 μm.

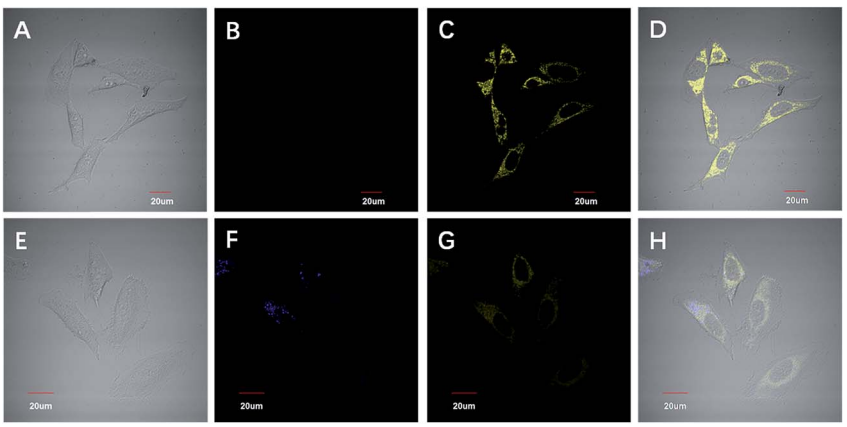

Fig. 7 Images of HeLa cells after incubation with IN-CZ (5 μM) in the absence and presence of $NaHSO_3$ (100 μM). (A and E) Bright-field; (B–D) are the images in the absence of $NaHSO_3$, blue channel, yellow channel and merged images in bright field; (F–H) are the images in the presence of $NaHSO_3$, blue channel, yellow channel and merged images in bright field. Excitation at 405 nm. Scale bar: 20 μm.

phosphate buffered saline. The images of yellow channel and red channel merged well in the HeLa cells. Along the red line, the intensity trends of Mito-tracker Red and **IN-CZ** have a high degree of overlap. Moreover, the Pearson's correlation coefficient was calculated to be 0.838, indicating that **IN-CZ** could localize in the mitochondria, which is one of the main organelles for generation of endogenous SO_2 *in vivo*. These results imply the potential capacity of **IN-CZ** for monitoring endogenous SO_2 in living cells.

To determine the favorable properties of the **IN-CZ** for monitoring SO_2 derivatives, we then evaluated the potential application of **IN-CZ** in living cells. As shown in Fig. 7, cells were incubated with **IN-CZ** (5 μM) for 10 min at 37 °C. There were nearly no fluorescence signals in the blue channel; obvious fluorescence signals can be observed in the yellow channel, which indicates the remarkable membrane permeability of the probe. Afterwards, cells were incubated with 100 μM of $NaHSO_3$ for 30 min at 37 °C, then the cells were incubated in culture media with **IN-CZ** (5 μM) for an additional 10 min at 37 °C. As we expected, the blue fluorescence channel gradually became bright and the yellow fluorescence channel became darkened. The obvious changes in ratiometric fluorescence responses generated from the blue channel and yellow channel in HeLa cells were observed. These results imply that **IN-CZ** could monitor SO_3^{2-}/HSO_3^- changes through the ratiometric fluorescence imaging in living cells.

4. Conclusion

In summary, we have presented a novel ratiometric fluorescent probe **IN-CZ** based on a hemicyanine dye platform. The probe could be used as a ratiometric fluorescent sensor for SO_3^{2-}/HSO_3^- anions in aqueous environment based on a Michael addition reaction. The probe displayed a fast reaction time, good sensitivity, and high selectivity for SO_3^{2-}/HSO_3^- over other reactive species, ROS, biologically relevant ions and biological mercaptans. Moreover, **IN-CZ** is a ratiometric fluorescent probe for the real-time monitoring of SO_3^{2-}/HSO_3^- changes through the ratiometric fluorescence imaging with mitochondria targeted in living cells with good permeability and low cytotoxicity. We expect that this design will be further developed as a good probe for SO_2 derivatives in realistic samples and biological applications.

Conflicts of interest

There are no conflicts to declare.

Acknowledgements

We gratefully acknowledge financial support from the National Natural Science Foundation of China (No. 21575015 and 21505004).

Notes and references

1 (*a*) T. M. Chen, W. G. Kuschner, J. Gokhale and S. Shofer, *Am. J. Med. Sci.*, 2007, **333**, 249–256; (*b*) M. Kampa and E. Gastanas, *Environ. Pollut.*, 2008, **151**, 362–367.
2 M. H. Stipanuk and I. Ueki, *J. Inherited Metab. Dis.*, 2011, **34**, 17–32.
3 (*a*) S. Iwasawa, Y. Kikuchi and Y. Nishiwaki, *J. Occup. Health*, 2009, **51**, 38–47; (*b*) M. Reist, P. Jenner and B. Halliwell, *FEBS Lett.*, 1998, **423**, 231–234.
4 (*a*) G. Li and N. Sang, *Ecotoxicol. Environ. Saf.*, 2009, **72**, 236–241; (*b*) G. L. Li, R. J. Li and Z. Q. Meng, *Eur. J. Pharmacol.*, 2010, **645**, 143–150.
5 (*a*) N. Sang, Y. Yun, H. Y. Li, L. Hou, M. Han and G. K. Li, *Toxicol. Sci.*, 2010, **114**, 226–236; (*b*) N. Sang, Y. Yun, G. Y. Yao, H. Y. Li, L. Guo and G. K. Li, *Toxicol. Sci.*, 2011, **124**, 400–413.
6 (*a*) Y. Liu, K. Li, M. Y. Wu, Y. H. Liu, Y. M. Xie and X. Q. Yu, *Chem. Commun.*, 2015, **51**, 10236–10239; (*b*) W. Xu, C. L. Teoh, J. J. Peng, D. D. Su, L. Yuan and Y. T. Chang, *Biomaterials*, 2015, **56**, 1–9.
7 (*a*) F. Y. Zhang, X. W. Liang, W. Z. Zhang, Y. L. Wang, H. L. Wang, Y. H. Mohammed, B. Song, R. Zhang and J. L. Yuan, *Biosens. Bioelectron.*, 2017, **87**, 1005–1011; (*b*) W. Z. Zhang, J. M. Zhang, H. L. Zhang, L. Y. Cao, R. Zhang, Z. Q. Ye and J. L. Yuan, *Talanta*, 2013, **116**, 354–360.
8 W. J. FAO, in *WHO food additives series*, World Health Organization, Geneva, 60th edn, 2009.
9 G. W. Monier-Williams, *Analyst*, 1927, **52**, 343–344.
10 (*a*) T. Yilmaz and G. Somer, *Anal. Chim. Acta*, 2007, **603**, 30–35; (*b*) C. S. Pundir and R. Rawal, *Anal. Bioanal. Chem.*, 2013, **405**, 3049–3062.
11 (*a*) P. W. West and G. Gaeke, *Anal. Chem.*, 1956, **28**, 1816–1819; (*b*) M. A. Segundo, A. O. Rangel, A. Cladera and C. Victor, *Analyst*, 2000, **125**, 1501–1505; (*c*) T. Williams, S. Mcelvany and E. Ighodalo, *Anal. Chim. Acta*, 1981, **123**, 351–354.
12 (*a*) P. Laura, D. L. Giuseppe and Q. Enrica, *Food Chem.*, 1998, **63**, 275–279; (*b*) R. F. McFeeters and A. O. Barish, *J. Agric. Food Chem.*, 2003, **51**, 1513–1517.
13 (*a*) D. Zydrunas and P. Audrius, *Electrophoresis*, 2002, **23**, 2439–2444; (*b*) J. Giedre, D. Zydrunas and P. Audrius, *J. Chromatogr. A*, 2001, **934**, 67–73.
14 L. Denise and B. Mauro, *Food Addit. Contam.*, 2001, **18**, 773–777.
15 (*a*) L. Tan, W. Lin, S. Zhu, L. Yuan and K. B. Zheng, *Org. Biomol. Chem.*, 2014, **12**, 4637–4643; (*b*) Y. Q. Sun, J. Liu, J. Zhang, T. Yang and W. Guo, *Chem. Commun.*, 2013, **49**, 2637–2639; (*c*) X. F. Yang, M. Zhao and G. Wang, *Sens. Actuators, B*, 2011, **152**, 8–13; (*d*) G. Y. Li, Y. Chen, J. Q. Wang, J. H. Wu, G. Gasser, L. N. Ji and H. Chao, *Biomaterials*, 2015, **63**, 128–136; (*e*) W. Q. Chen, X. J. Liu, S. Chen, X. Z. Song and J. Kang, *RSC Adv.*, 2015, **5**, 25409–25415; (*f*) S. Paul, K. Ghoshal, M. Bhattacharyya and D. K. Maiti, *ACS Omega*, 2017, **2**, 8633–8639; (*g*) M. G. Choi, J. Y. Hwang, S. Y. Eor and S. K. Chang, *Org. Lett.*, 2010, **12**, 5624–5627.

16 (*a*) J. Chan, S. C. Dodani and C. J. Chang, *Nat. Chem.*, 2012, **4**, 973; (*b*) Y. M. Yang, Q. Zhao, W. Feng and F. Y. Li, *Chem. Rev.*, 2013, **113**, 191–270; (*c*) J. J. Du, M. M. Hu, J. L. Fan and X. J. Peng, *Chem. Soc. Rev.*, 2012, **41**, 4511–4535; (*d*) F. Zhou, Y. Sultanbawa, H. Feng, Y. L. Wang, Q. T. Meng, Y. Wang, Z. Q. Zhang and R. Zhang, *J. Agric. Food Chem.*, 2019, **67**, 4375–4383; (*e*) W. Q. Chen, Q. Fang, D. L. Yang, H. Y. Zhang, X. Z. Song and J. Foley, *Anal. Chem.*, 2015, **87**, 609–616; (*f*) Y. Y. Ma, Y. H. Tang, Y. P. Zhao, S. Y. Gao and W. Y. Lin, *Anal. Chem.*, 2017, **89**, 9388–9393.

17 (*a*) J. Yang, K. Li, J. T. Hou, L. L. Li, C. Y. Lu, Y. M. Xie, X. Wang and X. Q. Yu, *ACS Sens.*, 2016, **1**, 166–172; (*b*) X. L. Zheng, H. Li, W. Feng, H. C. Xia and Q. H. Song, *ACS Omega*, 2018, **3**, 11831–11837; (*c*) G. Chen, W. Zhen, C. Y. Zhao, Y. X. Liu, T. Chen, Y. L. Li and B. Tang, *Anal. Chem.*, 2018, **90**, 12442–12448; (*d*) D. Y. Li, X. W. Tian, Z. Li, J. H. Zhang and X. B. Yang, *J. Agric. Food Chem.*, 2019, **67**, 3062–3067; (*e*) C. C. Gao, Y. Tian, R. B. Zhang, J. Jing and X. L. Zhang, *New J. Chem.*, 2019, **43**, 5255–5259; (*f*) Y. F. Wang, Q. T. Meng, R. Zhang, H. M. Jia, X. H. Zhang and Z. Q. Zhang, *Org. Biomol. Chem.*, 2017, **15**, 2734–2739.

18 (*a*) H. Chen, B. L. Dong, Y. H. Tang and W. Y. Lin, *Chem.–Eur. J.*, 2015, **21**, 11696–11700; (*b*) B. P. Guo, X. Z. Pan, Y. F. Liu, L. X. Nie, H. Z. Zhao, Y. Z. Liu, J. Jing and X. L. Zhang, *Sens. Actuators, B*, 2018, **256**, 632–638; (*c*) C. Y. Liu, C. X. Shao, H. F. Wu, B. P. Guo, B. C. Zhu and X. L. Zhang, *RSC Adv.*, 2014, **4**, 16055–16061.